Mon. Not. R. Astron. Soc. **342,** 513–518 (2003)

Emission lines of Na-like ions in spectra obtained with the Solar EUV Research Telescope and Spectrograph (SERTS)

F. P. Keenan,[1]★ A. C. Katsiyannis,[1] J. W. Brosius,[2,3] J. M. Davila[2] and R. J. Thomas[2]

[1]*Department of Pure and Applied Physics, Queen's University, Belfast BT7 1NN*
[2]*Laboratory for Astronomy and Solar Physics, Code 682, NASA's Goddard Space Flight Center, Greenbelt, MD 20771, USA*
[3]*Department of Physics, The Catholic University of America, Washington, DC 20064, USA*

Accepted 2003 February 19. Received 2003 February 17; in original form 2003 February 7

ABSTRACT

Theoretical emission-line ratios involving transitions in the 236–412 Å wavelength range are presented for the Na-like ions Ar VIII, Cr XIV, Mn XV, Fe XVI, Co XVII, Ni XVIII and Zn XX. A comparison of these with an extensive data set of the solar active region, quiet-Sun, subflare and off-limb observations, obtained during rocket flights by the Solar EUV Research Telescope and Spectrograph (SERTS), reveals generally very good agreement between theory and experiment. This indicates that most of the Na-like ion lines are reliably detected in the SERTS observations, and hence may be employed with confidence in solar spectral analyses. However, the features in the SERTS spectra at 236.34 and 300.25 Å, originally identified as the Ni XVIII 3p $^2P_{3/2}$–3d $^2D_{3/2}$ and Cr XIV 3p $^2P_{3/2}$–3d $^2D_{5/2}$ transitions, respectively, are found to be due to emission lines of Ar XIII (236.34 Å) and possibly S V or Ni VI (300.25 Å). The Co XVII 3s ^2S–3p $^2P_{3/2}$ line at 312.55 Å is always badly blended with an Fe XV feature at the same wavelength, but Mn XV 3s ^2S–3p $^2P_{1/2}$ at 384.75 Å may not always be as affected by second-order emission from Fe XII 192.37 Å as previously thought. On the other hand, we find that the Zn XX 3s ^2S–3p $^2P_{3/2}$ transition can sometimes make a significant contribution to the Zn XX/Fe XIII 256.43-Å blend, and hence care must be taken when using this feature as an Fe XIII electron density diagnostic. A line in the SERTS–89 active region spectrum at 265.00 Å has been re-assessed, and we confirm its identification as the Fe XVI 3p $^2P_{3/2}$–3d $^2D_{3/2}$ transition.

Key words: atomic data – Sun: activity – Sun: flares – ultraviolet: general.

1 INTRODUCTION

Emission lines arising from transitions in ions of the sodium isoelectronic sequence can be among the strongest observed in the solar ultraviolet spectrum (see, for example, Thomas & Neupert 1994). Flower & Nussbaumer (1975) first pointed out that line ratios involving Na-like ion transitions are potentially very useful electron temperature (T_e) diagnostics for the solar transition region and corona, while Laming & Feldman (1999) have noted that Na-like ions may be employed as abundance indicators. In addition, Feldman & Doschek (1977) have shown that Na-like ion emission-line ratios provide electron density (N_e) diagnostics for high-density laboratory plasmas, such as tokamaks.

In this paper we present new calculations of emission-line ratios for a number of Na-like ions between Ar VIII and Zn XX, observed in spectra obtained with the Solar EUV Research Telescope and Spectrograph (SERTS). We compare our results with an extensive SERTS data set comprising several quiet and active region spectra, plus a subflare and an off-limb area, to assess the importance of blending in the observations.

2 ADOPTED ATOMIC DATA AND THEORETICAL LINE RATIOS

The model ions for all the Na-like ions considered in the present paper consisted of the six energetically lowest LS states, namely 3s ^2S, 3p ^2P, 3d ^2D, 4s ^2S, 4p ^2P and 4d ^2D, making a total of 10 fine-structure levels. Energies for these were taken from Moore (1971), Corliss & Sugar (1982) and Shirai et al. (1987) for Ar VIII, Fe XVI and Ni XVIII, respectively, and Sampson et al. (1990) for all other ions. Test calculations including higher-lying levels were found to have a negligible effect on the theoretical line ratios considered in this paper, as also found by Doron et al. (2002).

Electron impact excitation rates for transitions among the levels discussed above were obtained from the following sources: Ar VIII – the **R**-matrix calculations of Kimura et al. (1998); Cr XIV, Mn XV and Co XVII – interpolated results of Keenan et al. (1996) based on **R**-matrix data; Fe XVI – **R**-matrix results of Eissner et al. (1999); Ni XVIII – **R**-matrix atomic data of Mohan, Sharma &

★E-mail: F.Keenan@qub.ac.uk

© 2003 RAS

Hibbert (1996); Zn XX – distorted-wave calculations of Sampson et al. (1990). Einstein A coefficients for allowed transitions were taken from Sampson et al. for all ions apart from Ar VIII and Fe XVI, where the results of Kimura et al. and Cornille et al. (1997), respectively, were adopted. Radiative rates for forbidden transitions from Charro, Bielińska-Waz & Martin (2000a) for Fe XVI, Charro, Martin & Bielińska-Waz (2000b) for Ni XVIII, and Godefroid et al. (1985) for other species, were also included in the model ions. However, we note that the inclusion of these data do not have a significant effect on the derived emission-line ratios.

As has been discussed by, for example, Seaton (1964), proton excitation may be important for transitions with small excitation energies, i.e. fine-structure transitions. However, test calculations for all the Na-like ions setting the proton rates for $^2P_{1/2}$–$^2P_{3/2}$ and $^2D_{3/2}$–$^2D_{5/2}$ equal to the electron rates, or 100 times these values, had a negligible effect on the level populations, showing this atomic process to be unimportant.

Using the atomic data discussed above in conjunction with the statistical equilibrium code of Dufton (1977), relative level populations and hence emission-line strengths were calculated for Ar VIII, Cr XIV, Mn XV, Fe XVI, Co XVII, Ni XVIII and Zn XX as a function of electron temperature and density. Details of the procedures involved and approximations made may be found in Dufton (1977) and Dufton et al. (1978).

In the present paper we consider the following line intensity ratios:

$$R_1 = I\left(3s\,^2S_{1/2}–3p\,^2P_{3/2}\right)/I\left(3s\,^2S_{1/2}–3p\,^2P_{1/2}\right),$$

$$R_2 = I\left(3p\,^2P_{1/2}–3d\,^2D_{3/2}\right)/I\left(3s\,^2S_{1/2}–3p\,^2P_{3/2}\right),$$

$$R_3 = I\left(3p\,^2P_{3/2}–3d\,^2D_{5/2}\right)/I\left(3s\,^2S_{1/2}–3p\,^2P_{3/2}\right),$$

$$R_4 = I\left(3d\,^2D_{5/2}–4p\,^2P_{3/2}\right)/I\left(3d\,^2D_{3/2}–4p\,^2P_{1/2}\right),$$

and

$$R_5 = I\left(3p\,^2P_{3/2}–3d\,^2D_{3/2}\right)/I\left(3s\,^2S_{1/2}–3p\,^2P_{3/2}\right)$$

as these involve the Na-like ion transitions which have been identified in the SERTS data sets (see Section 3). The wavelengths of these transitions for each Na-like ion are listed in Table 1, while in Table 2 we provide the theoretical values of the ratios at an electron density of $N_e = 10^{10}$ cm^{-3} and the temperature of maximum fractional abundance in ionization equilibrium, T_{max} (Mazzotta et al. 1998). However, we note that the ratios are insensitive to variations in the electron density for $N_e \leqslant 10^{13}$ cm^{-3}, and in addition vary slowly with electron temperature. For example, changing the temperature by ± 0.5 dex about T_{max} leads to a less than 1 per cent variation in R_1 for all the Na-like ions. Similarly, R_4 in Ar VIII, R_3 in Cr XIV and R_2 in Fe XVI vary by less than 1, 20 and 19 per cent, respectively, over the same temperature interval. Given typical uncertainties in the adopted atomic data of ± 10 per cent (see the references above), we would expect our line ratio calculations to be in error by at most 15 per cent. We note in passing that the theoretical line ratios in Table 2 are in very good agreement with those generated from the latest version (4.01) of the CHIANTI data base (Dere et al. 1997; Young et al. 2003).

Table 1. Emission lines of Na-like ions identified in SERTS spectra.

Ion	Transition	λ (Å)
Ar VIII	3d $^2D_{5/2}$–4p $^2P_{3/2}$	337.24
Ar VIII	3d $^2D_{3/2}$–4p $^2P_{1/2}$	338.18
Cr XIV	3p $^2P_{3/2}$–3d $^2D_{5/2}$	300.25
Cr XIV	3s $^2S_{1/2}$–3p $^2P_{3/2}$	389.85
Cr XIV	3s $^2S_{1/2}$–3p $^2P_{1/2}$	412.04
Mn XV	3s $^2S_{1/2}$–3p $^2P_{3/2}$	360.96
Mn XV	3s $^2S_{1/2}$–3p $^2P_{1/2}$	384.75
Fe XVI	3p $^2P_{1/2}$–3d $^2D_{3/2}$	251.07
Fe XVI	3p $^2P_{3/2}$–3d $^2D_{5/2}$	262.98
Fe XVI	3p $^2P_{3/2}$–3d $^2D_{3/2}$	265.00
Fe XVI	3s $^2S_{1/2}$–3p $^2P_{3/2}$	335.40
Fe XVI	3s $^2S_{1/2}$–3p $^2P_{1/2}$	360.75
Co XVII	3s $^2S_{1/2}$–3p $^2P_{3/2}$	312.55
Co XVII	3s $^2S_{1/2}$–3p $^2P_{1/2}$	339.54
Ni XVIII	3p $^2P_{3/2}$–3d $^2D_{3/2}$	236.34
Ni XVIII	3s $^2S_{1/2}$–3p $^2P_{3/2}$	291.99
Ni XVIII	3s $^2S_{1/2}$–3p $^2P_{1/2}$	320.56
Zn XX	3s $^2S_{1/2}$–3p $^2P_{3/2}$	256.43
Zn XX	3s $^2S_{1/2}$–3p $^2P_{1/2}$	288.16

Table 2. Line ratio designations for Na-like ions.

Ion	λ_1 (Å)	λ_2 (Å)	$R = I(\lambda_1)/I(\lambda_2)$	Theoretical value[a]
Ar VIII	337.24	338.18	R_4	1.8
Cr XIV	389.85	412.04	R_1	2.1
Cr XIV	300.25	389.85	R_3	0.072
Mn XV	360.96	384.75	R_1	2.1
Fe XVI	335.40	360.75	R_1	2.1
Fe XVI	251.07	335.40	R_2	0.047
Fe XVI	262.98	335.40	R_3	0.079
Fe XVI	265.00	335.40	R_5	0.0076
Co XVII	312.55	339.54	R_1	2.2
Ni XVIII	291.99	320.56	R_1	2.2
Ni XVIII	236.34	291.99	R_5	0.0047
Zn XX	256.43	288.16	R_1	2.2

Note. [a]Line intensity ratios (in energy units) calculated at an electron density of $N_e = 10^{10}$ cm^{-3}, and the electron temperature of maximum fractional abundance in ionization equilibrium (Mazzotta et al. 1998), namely $T_e = 10^{5.6}$ K (Ar VIII); $T_e = 10^{6.3}$ K (Cr XIV); $T_e = 10^{6.3}$ K (Mn XV); $T_e = 10^{6.4}$ K (Fe XVI); $T_e = 10^{6.5}$ K (Co XVII); $T_e = 10^{6.5}$ K (Ni XVIII); $T_e = 10^{6.6}$ K (Zn XX).

3 OBSERVATIONAL DATA

The solar spectra analysed here are those of several quiet and active regions, a small subflare, and an off-limb area, obtained with the SERTS instrument (Neupert et al. 1992). These spectra were recorded on Eastman Kodak 101–07 emulsion during SERTS rocket flights on 1989 May 5 (SERTS–89), 1991 May 7 (SERTS–91), 1993 August 17 (SERTS–93) and 1995 May 15 (SERTS–95). Unfortunately, the four subsequent SERTS flights all used an intensified CCD camera with limited spectral coverage, so that none of their observations were suitable for the present study. The spectral resolutions of the usable SERTS data sets are typically 50–80 mÅ (FWHM), while the spatial resolutions are approximately 7 arcsec (FWHM). Further details of the observations, and the wavelength and absolute flux calibration procedures employed in the data reduction, may be found in the following papers: SERTS–89, Thomas & Neupert (1994); SERTS–91 and SERTS–93, Brosius et al. (1996); SERTS–95, Brosius, Davila & Thomas (1998).

In Table 1 we list all of the Na-like ion emission lines identified in the SERTS spectral range by Thomas & Neupert (1994). Intensities of these features (where measurable) were determined using the spectrum synthesis package DIPSO (Howarth, Murray & Mills 1994) to fit Gaussian profiles to the SERTS observations. The intensities of the strongest Na-like ion transitions are listed in Table 3; the

Table 3. Intensities of the strongest Na-like ion emission lines in the SERTS data sets.

Ion	λ (Å)	89–AR[a]	89–SF	91–AR	91–QS	91–OL	93–AR	93–QS	95–AR
Ar VIII	337.24	24.8±7.4[b]	–	–	11.6 ± 2.7	–	–	–	16.2 ± 7.5
Cr XIV	389.85	83.6 ± 7.3	114.0 ± 7.3	35.5 ± 4.4	–	74.7 ± 18.7	55.9 ± 12.2	5.4 ± 1.5	–
Mn XV	360.96	86.8 ± 12.4	–	19.0 ± 12.9	–	33.0 ± 7.5	28.3 ± 4.3	–	–
Fe XVI	335.40	12 871 ± 1550	22 500 ± 1600	3380 ± 307	314.8 ± 25.3	1619 ± 123	4080 ± 368	163.4 ± 12.3	12 010 ± 984
Co XVII	312.55	85.6 ± 13.8	–	–	–	–	–	–	–
Ni XVIII	291.99	437.7 ± 41.0	1080 ± 90.0	230.0 ± 20.3	55.6 ± 16.2	17.2 ± 11.9	124.2 ± 28.3	–	482.0 ± 60.8
Zn XX	256.43	161.2 ± 51.3	267.0 ± 131.7	–	–	182.2 ± 84.0	–	–	220.6 ± 45.3

Notes. [a]The designations of the SERTS data sets are as follows: 89–AR, SERTS–89 active region spectrum; 89–SF, SERTS–89 subflare spectrum; 91–AR, SERTS–91 active region spectrum; 91–QS, SERTS–91 quiet-Sun spectrum; 91–OL, SERTS–91 off-limb spectrum; 93–AR, SERTS–93 active region spectrum; 93–QS, SERTS–93 quiet-Sun spectrum; 95–AR, SERTS–95 active region spectrum. [b]Intensities in units of erg cm^{-2} s^{-1} sr^{-1}.

observed intensities of the other lines may be inferred from these using the line ratios given in Tables 4–11. Also given as footnotes to these tables are the first-order bandpasses of the SERTS data sets. We note in passing that we have searched the SERTS spectra for Na-like ion emission lines in addition to those identified by Thomas & Neupert, but no convincing detections were forthcoming.

Observational uncertainties in the line intensities have been determined using methods discussed in detail by Thomas & Neupert (1994). The intensities and uncertainties quoted here are somewhat different from those originally reported in the papers referenced above, because the spectral data have been completely re-analysed by a standard fitting procedure to ensure consistency of the results. Also, a uniform factor of 1.24 has been applied here to all SERTS–89 intensities, reflecting a more recent re-evaluation of its absolute calibration scale. Even so, in all directly comparable cases, the resulting intensity ratios differ only slightly from those obtained using previously published data.

The quality of the observational data are illustrated in Figs 1–4, where we plot several portions of the SERTS spectra for a

Table 4. Emission-line ratios of Na-like ions in the SERTS–89 active region observations.[a]

Ion	Ratio	Observed	Theory
Ar VIII	R_4	2.0 ± 1.0	1.8
Cr XIV	R_1	2.2 ± 0.3	2.1
Cr XIV	R_3	0.59 ± 0.13	0.072
Mn XV	R_1	2.6 ± 0.5	2.1
Fe XVI	R_1	2.4 ± 0.4	2.1
Fe XVI	R_2	0.043 ± 0.006	0.047
Fe XVI	R_3	0.064 ± 0.011	0.079
Fe XVI	R_5	0.0085 ± 0.0015	0.0076
Co XVII	R_1	9.5 ± 6.3	2.2
Ni XVIII	R_1	2.3 ± 0.3	2.2
Ni XVIII	R_5	0.71 ± 0.21	0.0047
Zn XX	R_1	2.1 ± 0.8	2.2

Note. [a]The first-order SERTS–89 bandpass is 235.5–448.7 Å.

Table 5. Emission-line ratios of Na-like ions in the SERTS–89 subflare observations.[a]

Ion	Ratio	Observed	Theory
Cr XIV	R_1	2.3 ± 0.2	2.1
Cr XIV	R_3	0.52 ± 0.26	0.072
Fe XVI	R_1	2.2 ± 0.3	2.1
Fe XVI	R_2	0.049 ± 0.008	0.047
Fe XVI	R_3	0.064 ± 0.010	0.079
Ni XVIII	R_1	2.3 ± 0.3	2.2
Ni XVIII	R_5	0.19 ± 0.10	0.0047
Zn XX	R_1	4.2 ± 2.6	2.2

Note. [a]The first-order SERTS–89 bandpass is 235.5–448.7 Å.

Table 6. Emission-line ratios of Na-like ions in the SERTS–91 active region observations.[a]

Ion	Ratio	Observed	Theory
Cr XIV	R_1	2.2 ± 1.2	2.1
Cr XIV	R_3	0.14 ± 0.11	0.072
Mn XV	R_1	1.3 ± 0.9	2.1
Fe XVI	R_1	2.0 ± 0.2	2.1
Fe XVI	R_2	0.059 ± 0.022	0.047
Fe XVI	R_3	0.063 ± 0.012	0.079
Ni XVIII	R_1	2.4 ± 0.3	2.2

Note. [a]The first-order SERTS–91 bandpass is 231.8–445.3 Å. However, the intensity calibration below 274 Å is highly uncertain (Brosius et al. 1996).

Table 7. Emission-line ratios of Na-like ions in the SERTS–91 quiet-Sun observations.[a]

Ion	Ratio	Observed	Theory
Ar VIII	R_4	2.1 ± 1.6	1.8
Fe XVI	R_1	2.3 ± 0.3	2.1
Fe XVI	R_3	0.088 ± 0.021	0.079
Ni XVIII	R_1	3.5 ± 2.8	2.2

Note. [a]The first-order SERTS–91 bandpass is 231.8–445.3 Å. However, the intensity calibration below 274 Å is highly uncertain (Brosius et al. 1996).

Table 8. Emission-line ratios of Na-like ions in the SERTS–91 off-limb observations.[a]

Ion	Ratio	Observed	Theory
Cr XIV	R_1	2.6 ± 1.9	2.1
Mn XV	R_1	1.3 ± 0.9	2.1
Fe XVI	R_1	2.3 ± 0.2	2.1
Fe XVI	R_3	0.059 ± 0.013	0.079
Ni XVIII	R_1	4.4 ± 4.0	2.2
Zn XX	R_1	5.8 ± 3.4	2.2

Note. [a]The first-order SERTS–91 bandpass is 231.8–445.3 Å. However, the intensity calibration below 274 Å is highly uncertain (Brosius et al. 1996).

Table 9. Emission-line ratios of Na-like ions in the SERTS–93 active region observations.[a]

Ion	Ratio	Observed	Theory
Cr XIV	R_1	1.9 ± 0.8	2.1
Mn XV	R_1	0.73 ± 0.16	2.1
Fe XVI	R_1	2.0 ± 0.3	2.1
Fe XVI	R_3	0.051 ± 0.020	0.079
Ni XVIII	R_1	2.7 ± 0.7	2.2

Note. [a]The first-order SERTS–93 bandpass is 231.7–445.4 Å. However, the intensity calibration below 274 Å is highly uncertain (Brosius et al. 1996).

Table 10. Emission-line ratios of Na-like ions in the SERTS–93 quiet-Sun observations.[a]

Ion	Ratio	Observed	Theory
Cr XIV	R_1	2.6 ± 1.4	2.1
Fe XVI	R_1	2.1 ± 0.2	2.1

Note. [a]The first-order SERTS–93 bandpass is 231.7–445.4 Å. However, the intensity calibration below 274 Å is highly uncertain (Brosius et al. 1996).

Table 11. Emission-line ratios of Na-like ions in the SERTS–95 active region observations.[a]

Ion	Ratio	Observed	Theory
Ar VIII	R_4	0.9 ± 0.8	1.8
Fe XVI	R_2	0.043 ± 0.006	0.047
Fe XVI	R_3	0.072 ± 0.009	0.079
Ni XVIII	R_1	4.1 ± 2.2	2.2
Zn XX	R_1	12.1 ± 6.0	2.2

Note. [a]The first-order SERTS–95 bandpass is 234.1–447.7 Å. However, we note that this flight had a multilayer-coated grating that enhanced the second-order response while suppressing first order, making the intensity calibration very uncertain for wavelengths greater than 340 Å (Brosius et al. 1998).

variety of solar features measured on different flights of the rocket payload.

4 RESULTS AND DISCUSSION

In Tables 4–11 we list the Na-like ion emission-line ratios measured from the SERTS spectra, along with the associated 1σ errors. Also given in the tables are the theoretical ratios from Table 2. An inspection of the tables reveals that, for the few Ar VIII measurements available, there is good agreement between theory and observation, supporting the identification of the Ar VIII 337.24- and 338.18-Å lines in the SERTS spectra as suggested by Thomas & Neupert (1994).

For Cr XIV, the observed values of the R_1 ratio agree with theory, confirming the Thomas & Neupert (1994) identifications of the 389.85- and 412.04-Å transitions. However, all the measured R_3 ratios are much larger than theory, implying that the 300.25-Å line is not in fact due to Cr XIV, as originally suggested by Thomas & Neupert. Possible identifications for this feature include S V $3s3p\ ^1P$–$3p4p\ ^1D$ at 300.24 Å from the NIST Data base at http://physics.nist.gov/PhysRefData or Ni VI $3d^5\ ^2G_1$–$3d^4 4p\ ^2H_0$ at 300.27 Å from the Peter van Hoof's atomic line list at http://www.pa.uky.edu/~peter/atomic. Thomas & Neupert (1994) list the 384.75-Å line of Mn XV as being blended with Fe XII 192.37 Å, detected by SERTS in second order. However, the observed $R_1 = I(360.96\ \text{Å})/I(384.75\ \text{Å})$ ratio of Mn XV in the SERTS–89 active region spectrum is in good agreement with theory, showing that the Fe XII transition must make a negligible contribution to the 384.75-Å line flux, at least in this data set. For the other SERTS observations, the measured values of R_1 are up to a factor of ~3 smaller than theory, indicating that the 384.75-Å line intensity is mostly due to Fe XII in these instances.

There is generally excellent agreement between theory and observation for all the line ratios in Fe XVI, in contrast to the work of Thomas & Neupert (1994). For the SERTS–89 active region spectrum, these authors found a line intensity for the 265.00-Å feature

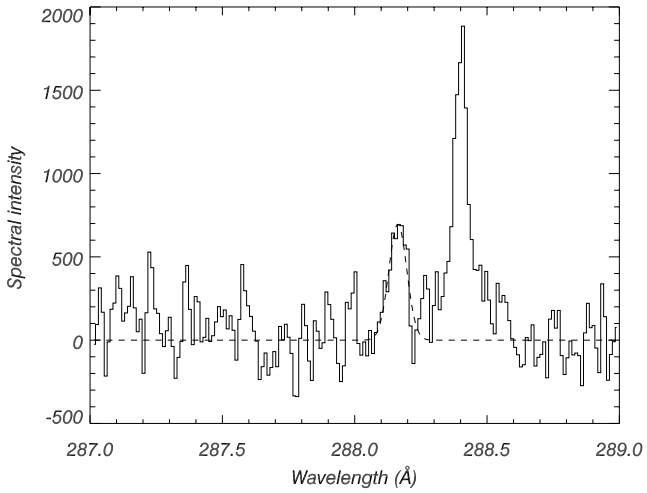

Figure 1. Plot of the SERTS–89 active region spectrum in the 287.0–289.0 Å wavelength range, where the spectral intensity is in units of erg $cm^{-2}\ s^{-1}\ sr^{-1}\ Å^{-1}$. The profile fit to the Zn XX 288.16-Å feature is shown by a dashed line. Also clearly visible in the figure is the S XII 288.40-Å emission line.

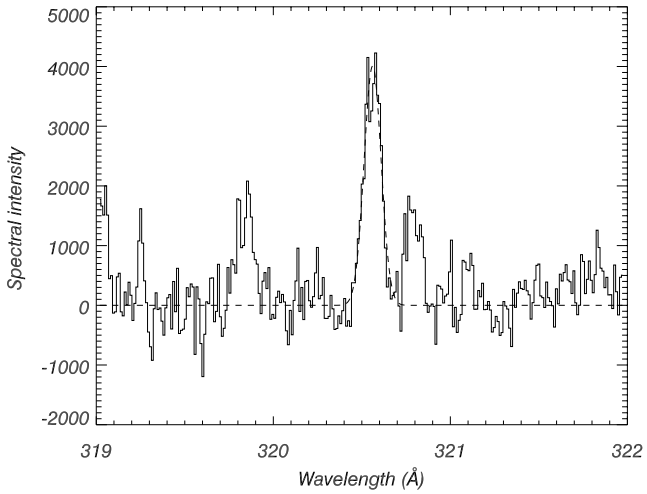

Figure 2. Plot of the SERTS–89 subflare spectrum in the 319.0–322.0 Å wavelength range, where the spectral intensity is in units of erg $cm^{-2}\ s^{-1}\ sr^{-1}\ Å^{-1}$. The profile fit to the Ni XVIII 320.56-Å feature is shown by a dashed line. Also clearly visible in the figure are the Si VIII 319.84-Å and Fe XIII 320.80-Å emission lines.

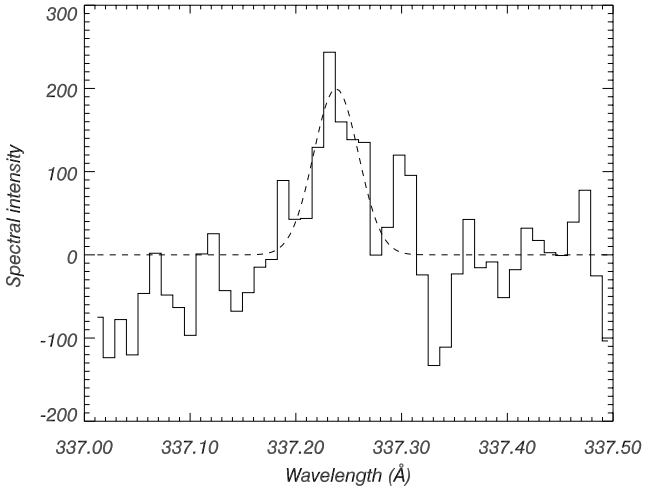

Figure 3. Plot of the SERTS–91 quiet-Sun spectrum in the 337.0–337.5 Å wavelength range, where the spectral intensity is in units of erg cm^{-2} s^{-1} sr^{-1} $Å^{-1}$. The profile fit to the Ar VIII 337.24-Å feature is shown by a dashed line.

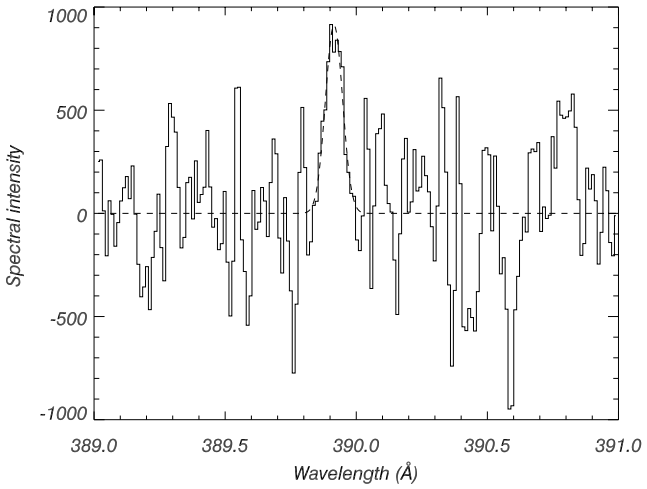

Figure 4. Plot of the SERTS–91 off-limb spectrum in the 389.0–391.0 Å wavelength range, where the spectral intensity is in units of erg cm^{-2} s^{-1} sr^{-1} $Å^{-1}$. The profile fit to the Cr XIV 389.85-Å feature is shown by a dashed line.

of $I(265.00\ Å) = 32.4 \pm 18.4$ erg cm^{-2} s^{-1} sr^{-1}, implying $R_5 = 0.0025 \pm 0.0014$, approximately a factor of 3 too low (see Table 2). This discrepancy for R_5 was also noted by Cornille et al. (1997) in their analysis of the SERTS–89 active region data set. However, we have carefully re-examined the original imaged observations for the 265.00-Å feature, and have corrected subtle flaws in 10 of the 1240 pixels that make up its averaged spectral line profile. In Fig. 5 we show the resulting portion of the corrected SERTS–89 active region spectrum containing the 265.00-Å line, along with our new fit to the feature. We now find $I(265.00\ Å) = 109.3 \pm 13.6$ erg cm^{-2} s^{-1} sr^{-1}, and hence a revised value of $R_5 = 0.0085 \pm 0.0015$, in excellent agreement with theory ($R_5 = 0.0076$) and the results of Young, Landi & Thomas (1998). An inspection of the figure reveals that the revised fit matches the corrected 265.00-Å line profile quite well, and so strongly supports its identification as the Fe XVI 3p $^2P_{3/2}$–3d $^2D_{3/2}$ transition. Further confirmation comes from the fact that the 265.00-Å feature has been well observed in solar flare spectra obtained with *Skylab* (where the Fe XVI lines are very strong), and shows good agreement between theory and experiment (Keenan et al. 1994).

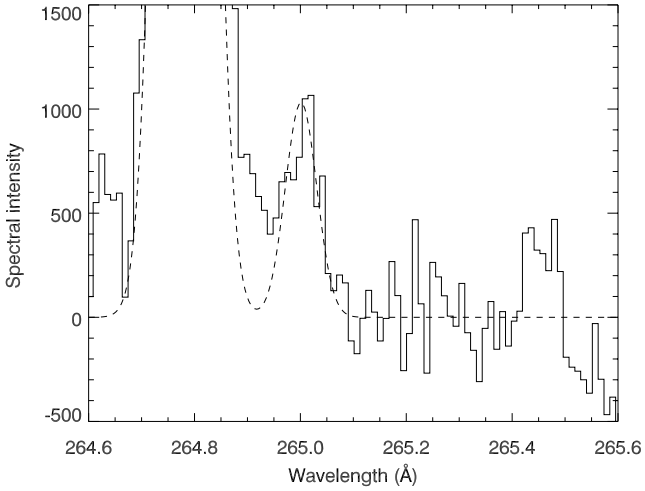

Figure 5. Plot of the corrected SERTS–89 active region spectrum in the 264.6–265.6 Å wavelength range, where the spectral intensity is in units of erg cm^{-2} s^{-1} sr^{-1} $Å^{-1}$. The profile fit to the Fe XVI 265.00-Å feature is shown by a dashed line. Also clearly visible in the figure is the Fe XIV 264.78-Å emission line.

Thomas & Neupert (1994) note that the 312.55-Å line of Co XVII is blended with Fe XV 312.55 Å. Our measurement of R_1 for Co XVII in Table 4 confirms this, with the observed ratio being a factor of ∼4 larger than theory, indicating that the Fe XV line is responsible for ∼75 per cent of the observed 312.55-Å flux.

In the case of Ni XVIII, there is very good agreement between theory and observation for R_1. However, the experimental values of R_5 are all far larger than predicted, indicating that the 236.34-Å line is not due to Ni XVIII, as previously identified by Thomas & Neupert (1994). Young et al. (1998) have also shown that this line cannot be Ni XVIII. Keenan et al. (1997) have noted that the line is likely to be Ar XIII $2s^22p^2\ ^3P_0$–$2s2p^3\ ^3D_1$, as originally suggested by Dere (1978). This identification is also supported by *Skylab* solar flare observations, where the intensity of this line is consistent with those of other Ar XIII features in the spectra (Keenan et al. 1993).

Thomas & Neupert (1994) note that the 256.43-Å line of Zn XX is blended with an Fe XIII transition at the same wavelength. This contrasts with the work of Landi (2002), who recommends the use of the 256.43-Å line in conjunction with other Fe XIII features as an electron density diagnostic. However, our measurement of $R_1 = I(256.43\ Å)/I(288.16\ Å)$ in Table 4 for the SERTS–89 active region indicates that, at least in this instance, Zn XX is responsible for most of the 256.43-Å intensity. In other SERTS data sets, such as the SERTS–89 subflare and SERTS–91 off-limb spectra, the observed values of R_1 are larger than theory, implying that Fe XIII is making a contribution to the 256.43-Å line blend, but that Zn XX is still a significant presence. Only in the SERTS–95 active region spectrum does Zn XX appear to make a negligible contribution to the 256.43-Å flux (Table 11). We therefore recommend that the 256.43-Å line is not employed as an Fe XIII density diagnostic, or at least is only used when the Zn XX 288.16-Å line is very weak, indicating that Zn XX 256.43 Å will not significantly affect measurements of the Fe XIII 256.43-Å line intensity.

In summary, our analysis of the SERTS data sets reveal generally very good agreement between theory and observation for the

Na-like ion transitions present in the spectra, indicating that the lines are reliably detected and are not seriously affected by blending. Most of the Na-like ion emission features may therefore be employed with confidence in solar spectral analyses, such as abundance studies (Doron et al. 2002).

ACKNOWLEDGMENTS

ACK acknowledges financial support from the Leverhulme Trust via grant F/00203/A. The SERTS rocket programme is funded under NASA RTOP 344-17-38. JWB acknowledges additional NASA support under contract NAS5-99145 and grant NAG5-11757. We thank P. van Hoof for use of his atomic line list.

REFERENCES

Brosius J.W., Davila J.M., Thomas R.J., Monsignori-Fossi B.C., 1996, ApJS, 106, 143
Brosius J.W., Davila J.M., Thomas R.J., 1998, ApJS, 119, 255
Charro E., Bielińska-Waz D., Martin I., 2000a, J. Phys. B, 33, 1855
Charro E., Martin I., Bielińska-Waz D., 2000b, A&AS, 146, 349
Corliss C., Sugar J., 1982, J. Phys. Chem. Ref. Data, 11, 135
Cornille M., Dubau J., Mason H.E., Blancard C., Brown W.A., 1997, A&A, 320, 333
Dere K.P., 1978, ApJ, 221, 1062
Dere K.P., Landi E., Mason H.E., Monsignori-Fossi B.C., Young P.R., 1997, A&AS, 125, 149
Doron R., Doschek G.A., Feldman U., Bhatia A.K., Bar-Shalom A., 2002, ApJ, 574, 504
Dufton P.L., 1977, Comput. Phys. Commun., 13, 25
Dufton P.L., Berrington K.A., Burke P.G., Kingston A.E., 1978, A&A, 62, 111
Eissner W., Galavís M.E., Mendoza C., Zeippen C.J., 1999, A&AS, 136, 385
Feldman U., Doschek G.A., 1977, J. Opt. Soc. Am., 67, 726
Flower D.R., Nussbaumer H., 1975, A&A, 42, 265
Godefroid M., Magnusson C.E., Zetterberg P.O., Joelsson I., 1985, Phys. Scr., 32, 125
Howarth I.D., Murray J., Mills D., 1994, Starlink User Note No. 50.15
Keenan F.P., Conlon E.S., Foster V.J., Aggarwal K.M., Widing K.G., 1993, Solar Phys., 145, 291
Keenan F.P., Conlon E.S., Foster V.J., Tayal S.S., Widing K.G., 1994, ApJ, 432, 809
Keenan F.P., Roche I.J., Foster V.J., Mohan M., 1996, Phys. Scr., 54, 163
Keenan F.P., Foster V.J., Mohan M., Widing K.G., 1997, Solar Phys., 171, 337
Kimura E., Ohsaki A., Nakazaki S., Itikawa Y., 1998, A&AS, 132, 99
Laming J.M., Feldman U., 1999, ApJ, 527, 461
Landi E., 2002, A&A, 382, 1106
Mazzotta P., Mazzitelli G., Colafrancesco S., Vittorio N., 1998, A&AS, 133, 403
Mohan M., Sharma R., Hibbert A., 1996, Phys. Scr., 54, 352
Moore C.E., 1971, Atomic Energy Levels, Natl Stand. Ref. Data, 35
Neupert W.M., Epstein G.L., Thomas R.J., Thompson W.T., 1992, Solar Phys., 137, 87
Sampson D.H., Zhang H.L., Fontes C.J., 1990, At. Data Nucl. Data Tables, 44, 209
Seaton M.J., 1964, MNRAS, 127, 191
Shirai T., Mori K., Sugar J., Wiese W.L., Nakai Y., Ozawa K., 1987, At. Data Nucl. Data Tables, 37, 235
Thomas R.J., Neupert W.M., 1994, ApJS, 91, 461
Young P.R., Landi E., Thomas R.J., 1998, A&A, 329, 291
Young P.R., Del Zanna G., Landi E., Dere K.P., Mason H.E., Landini M., 2003, ApJS, 144, 135

This paper has been typeset from a TEX/LATEX file prepared by the author.